Dalton Transactions

Accepted Manuscript

ROYAL SOCIETY OF CHEMISTRY

www.rsc.org/dalton

Dalton Transactions

ARTICLE

Structural phase transition in a multi-induced mononuclear Fe^{II} spin-crossover complex†

Received 00th January 20xx,
Accepted 00th January 20xx

DOI: 10.1039/x0xx00000x

www.rsc.org/

Yuan-Yuan Zhu,*[a] Chang-Wei Liu,[a] Ji Yin,[a] Zhao-Sha Meng,[b] Qian Yang,[b] Junhu Wang,[d] Tao Liu*[c] and Song Gao*[b]

Herein, we report the investigation of a mononuclear spin-crossover complex $[Fe^{II}L_2][ClO_4]_2$ (**L** = 2,6-bis{4,4-dimethyl-4,5-dihydrooxazol-2-yl}pyridine). This compound undergoes a structural phase transition around 173 K, accompanying with an abrupt spin-transition process. Interestingly, it exhibits a multi-induced spin-crossover behavior mediated by heat, light, pressure and solvent.

Introduction

Spin-transition (ST) complexes or spin-crossover (SCO) complexes are a fascinating class of compounds whose spin states can be switched *via* external perturbations such as heat, pressure, light, solvent and magnetic field, resulting in the changes of several physical properties including magnetic moment, color, dielectric constant and electrical resistance.[1] Since its first discovery more than four decedes years ago,[2] researches on SCO have received broad and sustained attention due to its potential applications in molecular switches, molecular sensors, data storage and display devices.[3] Recently, identification of novel multi-functional and multi-stimuli-responsive SCO compounds has become one of the most promising trends for the future applications in writing and erasing information at the single molecular level.[4,5] It is well known that heat, light and pressure can be used as external stimuli in the field of SCO, which can effectively tune the ligand-field strength and thus manipulate the SCO behavior.[6] In addition, guest solvent molecules usually induce weak intermolecular interactions in the frameworks of porous coordination polymers (CPs) and also have a influence on the ligand-field. In this context, solvent-containing CPs are another type of candidates with potential SCO behavior.[7] Similarly, several mononuclear complexes also display guest solvent mediated SCO behavior.[8] Among the ocean of SCO complexes, only a few compounds could exhibit strong coupling between the SCO and the structural phase transitions (SPT).[9,10] In these complexes, the spin-transition occurred with the accompany of space group change. Although some progress have been made in the past decade, complexes that display both SPT and multi-induced SCO behavior are still quite limited.[11]

Compounds containing pyridine-2,6-bis(oxazoline) (pybox) moiety are a family of privileged chiral ligands which have been extensively employed in asymmetric organic synthesis.[12] This type of ligands has also been used to construct luminescent and magnetic mononuclear complexes as well as CPs.[13,14] In view of their excellent luminescent properties and the structural similarity to the tridentate nitrogen ligands which were widely employed in constructing SCO complexes,[13,15] in this work the possibility to assemble SCO complexes containing the pybox type ligands was explored. We herein report a new mononuclear Fe^{II} SCO complex based on a pybox type ligand. The SCO behavior of this compound could be mediated by heat, light, pressure and solvent effectively. A structural phase transition associated with the spin-transition process of the compound was disclosed by the single-crystal X-ray diffraction analyses. This compound represents a new example of mononuclear complex with both SPT and multi-induced SCO behavior.

Results and discussion

Crystal structures of 1a and 1b

The pybox derivative **L** (2,6-bis{4,4-dimethyl-4,5-dihydrooxazol-2-yl}pyridine) bearing four methyl substituents was prepared by our modified method (see ESI for details). Two mononuclear Fe(II) complexes **1a** and **1b** with the general formula $(Fe^{II}L_2)(ClO_4)_2(MeCN)_n$ (n = 0 for **1a** and n = 1 for **1b**) were obtained from two different approaches. Mixing $Fe(ClO_4)_2$ and two equivalent of **L** in methanol then cooling the solution at −30 °C yielded solvent-free crystals of complex **1a**. Crystals of complex with acetonitrile solvent molecules co-crystallizing into the unit cell (**1b**)

[a] School of Chemistry and Chemical Engineering, Hefei University of Technology and Anhui Key Laboratory of Advanced Functional Materials and Devices, Hefei 230009, China. E-mail: yyzhu@hfut.edu.cn
[b] Beijing National Laboratory for Molecular Sciences, State Key Laboratory of Rare Earth Materials Chemistry and Applications, College of Chemistry and Molecular Engineering, Peking University, Beijing 100871, China. E-mail: gaosong@pku.edu.cn
[c] State Key Laboratory of Fine Chemicals, Dalian University of Technology, 2 Linggong Road, 116024, Dalian, China. E-mail: liutao@dlut.edu.cn
[d] Mössbauer Effect Data Center & Laboratory of Catalysts and New Materials for Aerospace, Dalian Institute of Chemical Physics, Chinese Academy of Sciences, 457 Zhongshan Road, Dalian 116023, China.

†Electronic Supplementary Information (ESI) available: Detailed synthetical procedure, characterization data, magnetic measurements and crystal structures. CCDC No: 1032872 (**1a** at 250 K), 1032876 (**1a** at 180 K), 1410363 (**1a** at 173 K), 1032884 (1a at 100 K) and 1032885 (**1b** at 100 K). See DOI: 10.1039/x0xx00000x

were obtained by slow diffusion of diethyl ether into the acetonitrile solution of **1a**.

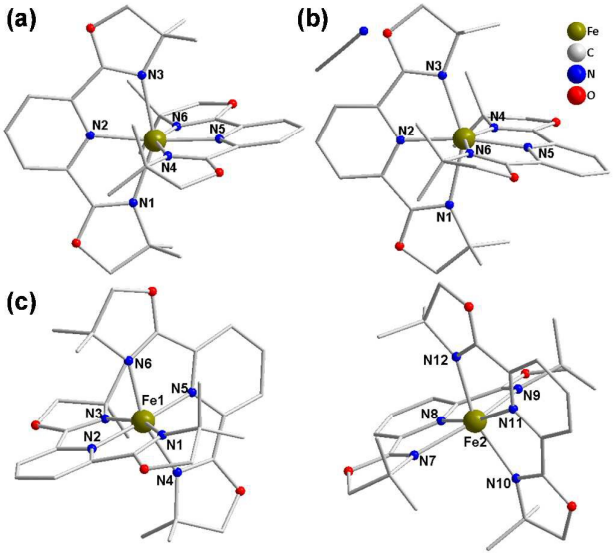

Fig. 1 Molecular structures of **1a** at 250 K (a), **1b** at 100 K (b) and **1a** at 100 K (c). Hydrogen atoms and counter ions of ClO_4^- were omitted for clarity.

Structural phase transition (SPT) phenomenon of **1a** was revealed through the single-crystal X-ray diffraction analysis at different temperatures. At 250 K, **1a** crystallized in the orthorhombic space group *P*bca with $Z = 8$. In the unit cell, the sole independent Fe^{II} centre is hexa-coordinated by two tridentate pybox ligands in a compressed octahedral environment. The conjugated planes of two ligands are approximately perpendicular to each other. Two ClO_4^- anions per Fe^{II} unit as counter anion are located in its periphery. The average Fe–N bond length of 2.172 Å at 250 K indicates the dominated HS state of Fe^{II} ions. Upon cooling to 180 K, the space group of **1a** was maintained and the Fe–N bond lengths just underwent a little contraction (2.161 Å in average). The orthorhombic unit cell was held till 174 K. However, the diffraction data indicated that the symmetry abruptly decreased to monoclinic space group $P2_1/c$ at 173 K and two symmetry independent Fe^{II} units could be found in the unit cell (Fig. 1c). This observation indicated that a SPT process happened around 173 K. Meanwhile, the SPT to low-temperature phase (LTP) caused the single crystal to fragment into several differently-oriented domains and yielded twinned crystals, resulting in a poor diffraction pattern and thus lowered the quality of the structural data obtained at LTP (Figure S4). However, the good diffraction data could be recovered when the crystal was back to high-temperature phase (HTP), showing this SPT process is dynamic and reversible. On the basis of the Fe–N bond length analysis and structural parameters (octahedral distortion parameter Σ and CShMs calculation of deviation from standard octahedron,[16,17] Tables 1 and 2), it can be distinguished that one Fe^{II} species (Fe1) is in LS state while another one (Fe2) is in HS state, demonstrating that **1a** adopts a 1HS : 1LS state population at LTP. At the critical phase transition temperature of 173 K, the spin-transition to LS of Fe1 ion started incoherently. Overall, it can be concluded that the SPT of **1a** is induced through an incomplete SCO process, which results in the appearance of crystallographically nonequivalent Fe^{II} ions in the asymmetric unit and thus leads to the space group change of the crystal.[9]

The single-crystal structure of **1b** was analysed at 100 K, which indicated that the molecule crystallized in the orthorhombic space group *P*bca with $Z = 8$ as well. Different from that of **1a**, one additional acetonitrile molecule per Fe^{II} species co-crystallized in the unit cell (Fig. 1(b)). The average Fe–N bond length of 2.191 Å indicated that the majority of Fe^{II} ions were in HS state at 100 K. It is notable that one pyridine ring of pybox ligand is deviated from the ligand plane (determined by three coordinated N atoms in the ligand), resulting in a bending angle of 9.24° (Figure S8). It demonstrates that the acetonitrile molecules strongly influence the molecular packing mode and cause the distortion of the coordination sphere of Fe^{II} ion. Previous researches have demonstrated that compounds containing HS Fe^{II} ions normally displayed significant deviation from the idealized octahedral symmetry.[18] The structural analyses of **1a** and **1b** confirmed this conclusion (Table 2).

Table 1. The selected bond lengths (Å) of FeN_6 sphere for **1a** and **1b** measured at different temperatures.

No	Fe–N1	Fe–N2	Fe–N3	Fe–N4	Fe–N5	Fe–N6
1a (250 K)	2.180(3)	2.104(3)	2.239(3)	2.191(3)	2.094(3)	2.224(3)
1a (180 K)	2.163(4)	2.097(3)	2.225(3)	2.209(3)	2.085(3)	2.184(3)
1a (173 K)	Fe1–N1	Fe1–N2	Fe1–N3	Fe1–N4	Fe1–N5	Fe1–N6
Fe1	2.11(1)	2.02(1)	2.15(1)	2.15(1)	2.04(1)	2.11(1)
1a (173 K)	Fe2–N7	Fe2–N8	Fe2–N9	Fe2–N10	Fe2–N11	Fe2–N12
Fe2	2.18(1)	2.09(1)	2.19(1)	2.22(1)	2.07(1)	2.18(1)
1a (100 K)	Fe1–N1	Fe1–N2	Fe1–N3	Fe1–N4	Fe1–N5	Fe1–N6
Fe1	2.01(1)	1.94(1)	2.01(1)	2.03(1)	1.88(1)	1.99(2)
1a (100 K)	Fe2–N7	Fe2–N8	Fe2–N9	Fe2–N10	Fe2–N11	Fe2–N12
Fe2	2.23(1)	2.12(2)	2.23(1)	2.20(1)	2.13(1)	2.22(2)
1b (100 K)	2.263(2)	2.122(2)	2.201(2)	2.217(2)	2.117(2)	2.225(2)

Table 2. The summary of structural parameters and spin state for **1a** and **1b** at different temperatures.

No	Σ(°)	Fe–$N_{average}$	S (O_h)	Spin state
1a (250 K)	135.83	2.172	4.756	HS
1a (180 K)	134.47	2.161	4.674	HS
1a (173 K) Fe1	117.20	2.096	3.653	HS→LS
1a (173 K) Fe2	134.80	2.156	4.735	HS
1a (100 K) Fe1	92.40	1.977	2.354	LS
1a (100 K) Fe2	140.90	2.189	5.045	HS
1b (100 K)	141.40	2.191	5.173	HS

Differential scanning calorimetry study

In order to confirm the SPT and SCO behavior of **1a**, the differential scanning calorimetry (DSC) measurement was performed in the temperature range 150–200 K with a warming/cooling rate of 5 K min^{-1}. The result is plotted in Fig. 2, which reveals an endothermic peak at 175 K (ΔH = 2.44 kJ mol^{-1} and ΔS = 13.9 J mol^{-1} K^{-1}) upon warming and an exothermic peak at 178 K (ΔH = 2.20 kJ mol^{-1} and ΔS = 12.4 J mol^{-1} K^{-1}) in the cooling process. These results indicate

that the SPT occurs around a narrow temperature range of 175 K to 178 K.

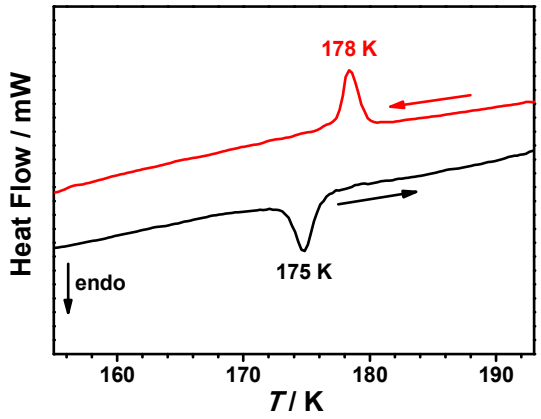

Fig. 2 Differential scanning calorimetry (DSC) profile of **1a** in the warming (black line) and cooling (red line) modes.

Mössbauer spectra study

The SCO behavior of **1a** was also investigated by ^{57}Fe Mössbauer spectra, which were recorded at 298 K and 77 K respectively to characterize the electronic states of the Fe^{II} centres in **1a** (Fig. 3). In high-temperature phase (HTP) at 298 K, only one quadrupole doublet was observed with Mössbauer parameters of δ (isomer shift) = 0.91 mm s^{-1} and ΔE_Q (quadrupole splitting) = 2.51 mm s^{-1}, which is characteristic of the HS Fe^{II} species. Upon cooling to 77 K, the quadrupole doublet of HS Fe^{II} species, with δ = 1.10 and ΔE_Q = 3.10 mm s^{-1}, was still visible, while an additional doublet with δ = 0.41 and ΔE_Q = 0.73 mm s^{-1}, corresponding to the LS Fe^{II} species, was prominent. The peak area ratio of the HS Fe^{II} to LS Fe^{II} species was 1:1 at 77 K, consistent with the result of the structural analyses above.

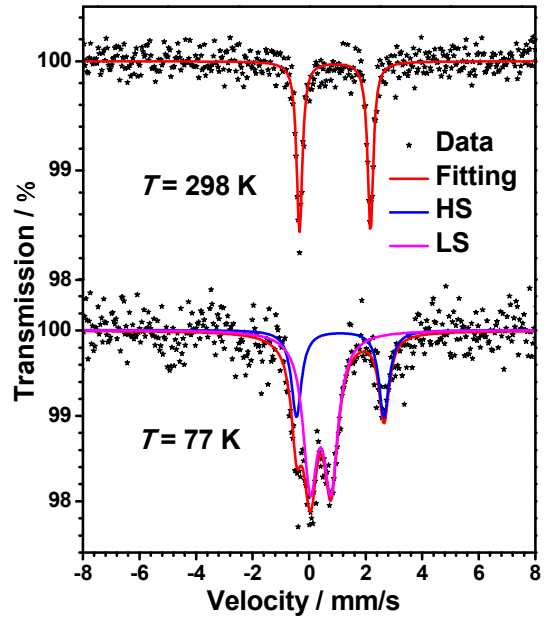

Fig. 3 Mössbauer spectra of **1a** recorded at 77 K and 298 K.

Magnetic properties study

To further determine the SCO behavior, magnetic measurements for **1a** and **1b** were performed on polycrystalline samples using Quantum-Design MPMS and PPMS magnetometers under a dc field of 5000 Oe in the range 10-300 K. The result demonstrated that **1a** underwent a spin-transition in a narrow temperature range with half of Fe^{II} centres transforming from HS to LS state (Fig. 4(a)). On the contrary, **1b** remained the totally HS state in the measured temperature range (Figure S9). Comprehensive investigation also revealed that the SCO behavior of **1a** could be mediated by heat, light, pressure and solvent.

The $\chi_M T$ *vs*. *T* plot of **1a** in cooling and warming modes is shown in Fig. 4(a). At 300 K, the $\chi_M T$ value is 3.60 cm^3 K mol^{-1}, consistent with the isolated HS Fe^{II} ion (*S* = 2) in an octahedral coordination environment. It remained roughly constant down to 190 K, while the $\chi_M T$ value decreased steeply from 3.50 cm^3 K mol^{-1} at 190 K to 1.91 cm^3 K mol^{-1} at 150 K in an *S*-shaped curve. The variation of $\chi_M T$ value implies that about half of HS Fe^{II} centres transform to LS Fe^{II} centres statistically. The temperature dependence of $d\chi_M T/dT$ *vs*. *T* curve (the inset of Fig. 4(a)) shows two peaks at 162 K and 176 K, respectively, revealing a two-step spin-transition process in this narrow temperature range. Further cooling to below 10 K led to a second decrement due to the zero-field splitting effect of the remained HS Fe^{II} centres with an *S* = 2 spin state. The warming/cooling cycle experiment did not show thermal hysteresis, indicating the fast relaxation dynamics of spin-transition in this compound.

In order to explore the possible LIESST effect, photomagnetic properties of **1a** were measured. Solid UV-vis spectrum of **1a** showed a broad absorption band around 540 nm (Figure S10). Therefore in the following photomagnetic experiment a green light (λ = 532 nm) laser source was chosen to irradiate the powder sample of **1a** to match the absorption band. Upon the light irradiation at 2.2 K for 12 h, a significant increment of the $\chi_M T$ value was observed, as a result of the photo-induced spin-transition process from diamagnetic LS Fe^{II} species to metastable paramagnetic HS Fe^{II} species (the red line in Fig. 4(a)). After irradiation, the $\chi_M T$ value increased steeply to reach a maximum value of 2.91 cm^3 K mol^{-1} at 40 K, corresponding to about 60% LS Fe^{II} species converting into HS state at low temperature. The photo-induced metastable HS state could be retained in the low temperature range but relaxed to the LS state by warming to 100 K. Overall, the magnetization of **1a** could be manipulated by light irradiation and be recovered with a thermal process at high temperature.

The influence of hydrostatic pressure on the SCO behavior of **1a** was also investigated.[19] The $\chi_M T$ *vs*. *T* curves measured under different pressures (0.15–0.22 GPa) are shown in Fig. 4(b). At ambient pressure the spin transition curve shows that the value of T_C (T_C: the temperature for half spin-transition of the SCO process) is about 170 K (Fig. 3(a)). When the hydrostatic pressure increases from 0.15 GPa to 0.22 GPa, the spin transition curves shift toward higher temperature range gradually. The T_C is about 240 K at 0.22 GPa, with a variation of 70 K. Different from the fast relaxation dynamics at ambient pressure, significant thermal hysteresis loop can be observed under a hydrostatic pressure. These pressure experiments demonstrate that the external pressure can

manipulate the ligand-field strength of **1a** and thus tune the SCO behavior in a controlled manner.

Compounds **1a** and **1b** display entirely distinct magnetic properties. The SCO behavior disappeared when acetonitrile solvent molecules crystallized in the unit cell. It would be interesting to observe the possibility of dynamics controlling the SCO behavior with guest solvent. By warming the powder sample of **1b** in quartz tube at 150 °C under a N_2 atmosphere, the acetonitrile molecules entrapped in the crystals could be removed completely. The powder XRD profile of a sample of desolvated **1b** (named **1b'**) matches well to that of **1a** (Figure S12). It is therefore not surprising to observe the SCO behavior in **1b'** (Figure S14). In addition, **1a** could also be transformed into **1b** by recrystallization in a mixed solvent of acetonitrile and ether. This experiment reveals that the acetonitrile solvent can serve as a dynamic molecular switch to manipulate the SCO behavior of this complex.

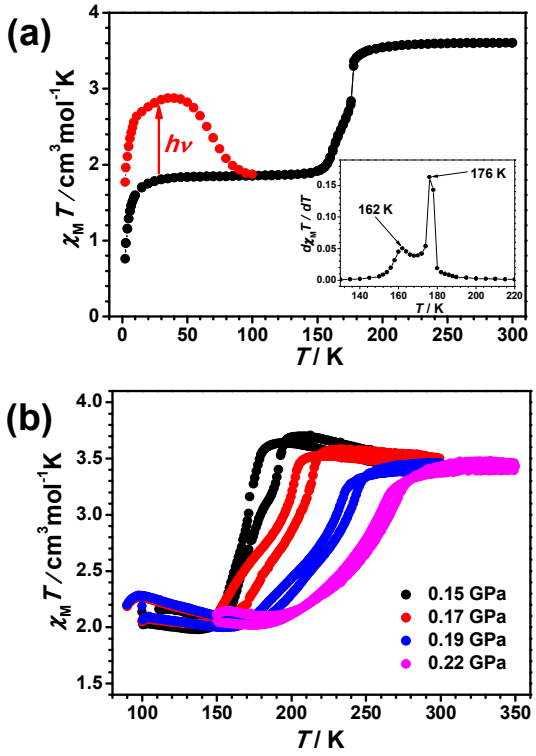

Fig. 4(a) Plot of $\chi_M T$ *vs. T* for **1a**. Red plots: the results of LIESST experiment at low temperature. Inset: Plot of $d\chi_M T/dT$ *vs. T*, which indicates the two-step SCO transition in the narrow range 140–190 K; **(b)** Plot of $\chi_M T$ *vs. T* under different pressures for **1a**.

Conclusions

In summary, a mononuclear Fe^{II} SCO complex was synthesized by using pybox type ligand. This compound exhibited a multi-induced SCO behavior mediated by heat, light, pressure and solvent. A structural phase transition accompanied with the abrupt and incomplete spin transition process was also observed. It represents a new example of the SPT and multi-induced SCO compound and show potential applications in the spin switch device at single molecular level. Further comprehensive studies of these type ligands in constructing novel SCO complexes is in progress and will be reported in the near future.

Experimental

Materials and synthesis

All solvents and reagents for synthesis were of analytical grade and used as received from commercial sources. The synthesis and characterization of pybox ligand **L** (2,6-bis{4,4-dimethyl-4,5-dihydrooxazol-2-yl}pyridine) is listed in ESI.

Physical measurements

Magnetic properties measurement. Magnetic susceptibility data were collected using a Quantum Design MPMS XL-5 or PPMS-9T (EC-II) SQUID magnetometer. Measurements for all the samples were performed on microcrystalline powder restrained by a parafilm and loaded in a capsule. The magnetic susceptibility data were corrected for the diamagnetism of the samples using Pascal constants[20] and the sample holder and parafilm by corrected measurement.

Photomagnetic measurement. A powdered sample, which was spread on a commercial transparent adhesive tape, was used to study the photo-effects. The weight of the sample on the tape was determined by measuring the weight of the tape before and after spreading the sample and determining the difference. The photo irradiation of the samples was performed at 2.2 K with a laser diode pumped Nd:YAG laser (λ = 532 nm, 30 mW/cm^2, 12 h). The temperature dependent magnetization was measured before and after irradiation in the temperature range from 2 to 100 K. Furthermore, from these magnetization values and the sample weight, the difference in the $\chi_M T$ values before and after irradiation ($\Delta\chi_M T$) were calculated. A scan rate of 0.3 K min^{-1} was used following the *T*(LIESST) procedure.[21]

Magnetic susceptibility measurements under hydrostatic pressure. The variable-temperature magnetic susceptibility measurements under hydrostatic pressure were performed on microcrystalline powder of the complex by using a Quantum Design MPMS XL-5 SQUID magnetometer. The hydrostatic pressure cell was made of hardened beryllium bronze with silicon oil as the pressure transmitting medium operates in the pressure range 0.15 Pa $\leq p \leq$ 0.22 GPa (accuracy$\approx\pm$0.025 GPa). Cylindrically shaped powder sample holders with 1 mm in diameter and 5–7 mm in length were used. The pressure was measured using the pressure dependence of the superconducting transition temperature of a built-in pressure sensor made of high purity tin.[22] Experimental data were corrected for diamagnetism using Pascal's constants.[20]

Mössbauer spectra measurements. Mössbauer spectra (isomer shift versus metallic iron at room temperature) were measured using a Wissel MVT-1000 Mössbauer spectrometer with a ^{57}Co/Rh source in the transmission mode. Measurements at low temperature were performed using a closed-cycle helium refrigerator cryostat (Iwatani Co., Ltd.).

Calorimetric studies. Differential scanning calorimetry (DSC) was carried out with a DSC 823e (Mettler Toledo) at a cooling and warming rate of 5 °C/min.

Other characterization. The ^{1}H NMR spectra were recorded using a Bruker 400 and 600 MHz {H} spectrometer. Elemental analysis of carbon, nitrogen and hydrogen was performed using an Elementary Vario EL analyzer. Solid UV-vis spectra were recorded using Hatachi 4100 spectrophotometer. Powder X-ray diffraction (XRD) patterns were obtained in the range of $5° < 2\vartheta < 50°$ at room temperature against the bulk crystalline samples on a Rigaku Dmax 2000 diffractometer with Cu Kα radiation in a flat plate geometry.

X-ray Data Collection and Structure Determinations

Crystal suitable for X-ray diffraction were covered in a thin layer of hydrocarbon oil, mounted on a glass fiber attached to a copper pin, and placed under an N_2 cold stream. Data for **1a** at 100 K, 180 K, and 250 K, and **1b** at 100 K was collected on an Rigaku SuperNova Atlas Dual system with a (Mo) microfocus source and focusing multilayer mirror optics (λ = 0.71073 Å). Intensities were collected using CrysAlisPro (Rigaku, Version 1.171.36.32) and absorption corrections were applied using 'multi-scan' method. Data for **1a** at 173 K were carried on a Saturn724+ CCD diffractometer with Confocal-monochromator Mo-Kα radiation (λ = 0.71073 Å). Intensities were collected using CrystalClear (Rigaku Inc., 2008) technique and absorption corrections were applied using the 'multi-scan' method.

Crystal structures were solved by the direct methods and refined on F^2 by full-matrix least squares using SHELXTL-97 and Olex 2 (version 1.2.6).[23,24] All non-hydrogen atoms were refined with anisotropic thermal parameters, while all hydrogen atoms were placed at calculated positions and refined using a riding model. Full crystallographic tables for five structures are presented in the ESI (Table S1).

Synthetic procedures

Preparation of $[Fe(L)_2](ClO_4)_2$ (1a). The single crystals were obtained by recrystallization at low temperature. To a solution of **L** (55 mg, 0.2 mmol) in 5 mL of methanol was added a solution of $Fe(ClO_4)_2{\cdot}6H_2O$ (36 mg, 0.1 mmol) in 5 mL of methanol under stirring, the color of solution turned to violet immediately and no precipitate formed. The solution was sealed and placed in a glovebox at −30 °C under a N_2 atmosphere. After three days, dark red cubic crystals (56 mg, 70%) were obtained, which were suitable for X-ray crystallographic analysis. Anal. Calcd for $C_{30}H_{38}Cl_2FeN_6O_{12}$: C, 44.96; H, 4.78; N, 10.49. Found: C, 45.07; H, 4.82; N, 10.38. IR (single crystal): ν = 3080 (w), 2976 (w), 2934 (w), 2874 (w), 2017 (w), 1869 (w), 1638 (w), 1619 (w), 1570 (m), 1483 (w), 1463 (w), 1401 (m), 1381 (m), 1371 (w), 1333 (w), 1299 (w), 1251 (w), 1219 (w), 1205 (w), 1173 (w), 1150 (w), 1093 (s), 1026 (w), 980 (w), 936 (m), 835 (w), 753 (w), 687 (w), 623 (m).

Preparation of $[Fe(L)_2](ClO_4)_2{\cdot}MeCN$ (1b). The single crystals were obtained by vapor diffusion. To a solution of **L** (55 mg, 0.2 mmol) in 5 mL of methanol was added a solution of $Fe(ClO_4)_2{\cdot}6H_2O$ (36 mg, 0.1 mmol) in 5 mL of methanol under stirring. The violet transparent solution was stirred for about 10 minutes and concentrated under reduced pressure. The resulting residue was dissolved in acetonitrile (5 mL) and then ether (about 10 mL) was allowed to vapor diffuse into the solution during a period of three days under a N_2 atmosphere. Dark red cubic crystals (67 mg, 80%) were obtained, which were suitable for X-ray crystallographic analysis. Anal. Calcd for $C_{32}H_{41}Cl_2FeN_7O_{12}$: C, 45.62; H, 4.91; N, 11.64. Found: C, 45.62; H, 4.95; N, 11.78. IR (single crystal): ν = 3084 (w), 2983 (w), 2939 (w), 2875 (w), 2247 (w), 2023 (w), 1641 (m), 1621 (w), 1572 (m), 1484 (w), 1462 (w), 1402 (m), 1381 (m), 1336 (w), 1297 (m), 1255 (w), 1220 (w), 1202 (m), 1147 (w), 1097 (s), 1026 (w), 982 (w), 936 (w), 840 (w), 830 (w), 758 (w), 746 (w), 686 (w), 675 (w), 624 (m).

Acknowledgements

This work was supported in part by the NSFC (21071008, 21321001, 21371043 and 21302035), the National Basic Research Program of China (2010CB934601, 2013CB933401) and the Fundamental Research Funds for the Central Universities. We thank Dr. Ning Li (Rigaku) for help in structure refinement and Dr. Hua-Gao Fang (HFUT) for help in DSC measurement. We grateful acknowledge Prof. Xin Zhao (SIOC) for helpful discussions.

Notes and references

1 (a) *Spin Crossover in Transition Metal Compounds I–III*, ed. P. Gütlich and H. A. Goodwin, *Top. Curr. Chem.*, 2004; vol. 233–235; (b) M. A. Halcrow, Spin-crossover materials: properties and applications; John Wiley & Sons, Ltd.: New York, 2013.

2 (a) L. Cambi and L. Szego, Ber. *Dtsch. Chem. Ges.*, 1931, **64**, 2591. (b) L. Cambi and A. Cagnasso, *Atti. Accad. Naz. Lincei.*, 1931, **13**, 809.

3 (a) J. A. Real, E. Andres, M. C. Muñoz, M. Julve, T. Granier, A. Bousseksou and F. Varret, *Science*, 1995, **268**, 265; (b) O. Kahn and C. J. Martinez, *Science*, 1998, **279**, 44; (c) A. Bousseksou, G. Molnár, L. Salmon and W. Nicolazzi, *Chem. Soc. Rev.*, 2011, **40**, 3313; (d) H. J. Shepherd, I. A. Gural'skiy, C. M. Quintero, S. Tricard, L. Salmon, G. Molnár and A. Bousseksou, *Nat. Commun.*, 2013, **4**, 2607; (e) A. B. Gaspar and M. Seredyuk, *Coord. Chem. Rev.*, 2014, **268**, 41.

4 (a) C. J. Kepert, *Chem. Commun.*, 2006, 695; (b) O. Sato, J. Tao and Y.-Z. Zhang, *Angew. Chem. Int. Ed.*, 2007, **46**, 2152; (c) S.-i. Ohkoshi, K. Imoto, Y. Tsunobuchi, S. Takano and H. Tokoro, *Nat. Chem.*, 2011, **3**, 564; (d) X. Feng, C. Mathonière, I.-R. Jeon, M. Rouzières, A. Ozarowski, M. L. Aubrey, M. I. Gonzalez, R. Clérac and J. R. Long, *J. Am. Chem. Soc.*, 2013, **135**, 15880; (e) C. Mathonière, H.-J. Lin, D. Siretanu, R. Clérac and J. M. Smith, *J. Am. Chem. Soc.*, 2013, **135**, 19083; (f) T. Liu, H. Zheng, S. Kang, Y. Shiota, S. Hayami, M. Mito, O. Sato, K. Yoshizawa and C. Duan, *Nat. Commun.*, 2013, **4**, 3826.

5 (a) O. Sato, T. Iyoda, A. Fujishima and K. Hashimoto, *Science*, 1996, **272**, 704; (b) M. C. Muñoza and J. A. Real, *Coord. Chem. Rev.*, 2011, **255**, 2068; (c) G. Agustí, A. L. Thompson, A. B. Gaspar, M. C. Mŭnoz, A. E. Goeta, J. A. Rodríguez-Velamazán, M. Castro, R. Burriel and J. A. Real, *Dalton Trans.*, 2008, 642; (d) J. R. Thompson, R. J. Archer, C. S. Hawes, A. Ferguson, A. Wattiaux, C. Mathonière, R. Clérac and P. E. Kruger, *Dalton Trans.*, 2012, **41**, 12720; (e) A. Mondal, Y. Li, L.-M.

Chamoreau, M. Seuleiman, L. Rechignat, A. Bousseksou, M.-L. Boillot and R. Lescouëzec, *Chem. Commun.*, 2014, **50**, 2893; (f) G. A. Craig, J. S. Costa, O. Roubeau, S. J. Teat, H. J. Shepherd, M. Lopes, G. Molnár, A. Bousseksou and G. Aromí, *Dalton Trans.*, 2014, **43**, 729.

6 (a) A. Galet, A. B. Gaspar, M. C. Muñoz, G. V. Bukin, G. Levchenko and J. A. Real, *Adv. Mater.*, 2005, **17**, 2949; (b) L. Zhang, G.-C. Xu, H.-B. Xu, T. Zhang, Z.-M. Wang, M. Yuan and S. Gao, *Chem. Commun.*, 2010, **46**, 2554; (c) X. Bao, P.-H. Guo, W. Liu, J. Tucek, W.-X. Zhang, J.-D. Leng, X.-M. Chen, I. y. Gural'skiy, L. Salmon, A. Bousseksou and M.-L. Tong, *Chem. Sci.*, 2012, **3**, 1629; (d) J.-B. Lin, W. Xue, B.-Y. Wang, J. Tao, W.-X. Zhang, J.-P. Zhang and X.-M. Chen, *Inorg. Chem.*, 2012, **51**, 9423.

7 (a) G. J. Halder, C. J. Kepert, B. Moubaraki, K. S. Murray and J. D. Cashion, *Science*, 2002, **298**, 1762; (b) V. Niel, A. L. Thompson, M. C. Munoz, A. Galet, A. E. Goeta and J. A. Real, *Angew. Chem.Int. Ed.*, 2003, **42**, 3760; (c) S. M. Neville, G. J. Halder, K. W. Chapman, M. B. Duriska, B. Moubaraki, K. S. Murray and C. J. Kepert, *J. Am. Chem. Soc.*, 2009, **131**, 12106; (d) X.-Y. Chen, H.-Y. Shi, R.-B. Huang, L.-S. Zheng and J. Tao, *Chem. Commun.*, 2013, **49**, 10977.

8 (a) B. Li, R.-J. Wei, J. Tao, R.-B. Huang, L.-S. Zheng and Z. Zheng, *J. Am. Chem. Soc.*, 2010, **132**, 1558; (b) R.-J. Wei, J. Tao, R.-B. Huang and L.-S. Zheng, *Inorg. Chem.*, 2011, **50**, 8553; (c) J. S. Costa, S. Rodríguez-Jiménez, G. A. Craig, B. Barth, C. M. Beavers, S. J. Teat and G. Aromí, *J. Am. Chem. Soc.*, 2014, **136**, 3869.

9 H. Shatruk, H. Phan, B. A. Chrisostomo and A. Suleimenova, *Coord. Chem. Rev.*, 2015, **62-73**, 289.

10 (a) D. Chernyshov, M. Hostettler, K. W. Türnroos and H. Bürgi, *Angew. Chem. Int. Ed.*, 2003, **42**, 3825; (b) S. Hayami, K. Murata, D. Urakami, Y. Kojima, M. Akita and K. Inoue, *Chem. Commun.*, 2008, 6510; (c) C.-F. Sheu, S.-M. Chen, S.-C. Wang, G.-H. Lee, Y.-H. Liu and Y. Wang, *Chem. Commun.*, 2009, 7512; (d) M. Nihei, H. Tahira, N. Takahashi, Y. Otake, Y. Yamamura, K. Saito and H. Oshio, *J. Am. Chem. Soc.*, 2010, **132**, 3553; (e) M. Griffin, S. Shakespeare, H. J. Shepherd, C. J. Harding, J.-F. Létard, C. Desplanches, A. E. Goeta, J. A. K. Howard, A. K. Powell, V. Mereacre, Y. Garcia, A. D. Naik, H. Müller-Bunz and G. G. Morgan, *Angew. Chem. Int. Ed.*, 2011, **50**, 896; (f) A. Lennartson, A. D. Bond, S. Piligkos and C. J. McKenzie, *Angew. Chem. Int. Ed.*, 2012, **51**, 11049; (g) T. D. Roberts, F. T. Tuna, T. L. Malkin, C. A. Kilner and M. A. Halcrow, *Chem. Sci.*, 2012, **3**, 349; (h) Z.-Y. Li, J.-W. Dai, Y. Shiota, K. Yoshizawa, S. Kanegawa and O. Sato, *Chem.–Eur. J.*, 2013, **19**, 12948; (i) T. D. Roberts, M. A. Little, F. Tuna, C. A. Kilner and M. A. Halcrow, *Chem. Commun.*, 2013, **49**, 6280; (j) J. Luan, J. Zhou, Z. Liu, B. Zhu, H. Wang, X. Bao, W. Liu, M.-L. Tong, G. Peng, H. Peng, L. Salmon and A. Bousseksou, *Inorg. Chem.*, 2015, **54**, 5145.

11 (a) N. Bréfuel, H. Watanabe, L. Toupet, J. Come, N. Matsumoto, E. Collet, K. Tanaka and J.-P. Tuchagues, *Angew. Chem. Int. Ed.*, 2009, **48**, 9304; (b) N. Bréfuel, E. Collet, H. Watanabe, M. Kojima, N. Matsumoto, L. Toupet, K. Tanaka and J.-P. Tuchagues, *Chem.–Eur. J.*, 2010, **16**, 14060; (c) K. D. Murnaghan, C. Carbonera, L. Toupet, M. Griffin, M. M. Dîrtu, C. Desplanches, Y. Garcia, E. Collet, Jean-F. Létard and G. G. Morgan, *Chem.–Eur. J.*, 2014, **20**, 5613.

12 (a) G. Desimoni, G. Faita and P. Quadrelli, *Chem. Rev.*, 2003, **103**, 3119; (b) S. E. Schaus and E. N. Jacobsen, *Org. Lett.*, 2000, **2**, 1001; (c) C. Wei and C.-J. Li, *J. Am. Chem. Soc.*, 2002, **124**, 5638; (d) E. Milczek, N. Boudet and S. Blakey, *Angew. Chem. Int. Ed.*, 2008, **47**, 6825.

13 (a) A. de Bettencourt-Dias, S. Viswanathan and A. Rollett, *J. Am. Chem. Soc.*, 2007, **129**, 15436; (b) J. Yuasa, T. Ohno, K. Miyata, H. Tsumatori, Y. Hasegawa and T. Kawai, *J. Am. Chem. Soc.*, 2011, **133**, 9892; (c) A. de Bettencourt-Dias, P. S. Barber and S. Bauer, *J. Am. Chem. Soc.*, 2012, **134**, 6987.

14 (a) S. Chorazy, K. Nakabayashi, K. Imoto, J. Mlynarski, B. Sieklucka and S.-i. Ohkoshi, *J. Am. Chem. Soc.*, 2012, **134**, 16151; (b) Y.-Y. Zhu, C. Cui, N. Li, B.-W. Wang, Z.-M. Wang and S. Gao, *Eur. J. Inorg. Chem.*, 2013, 3101; (c) N. Liu, L.-H. Jia, Z.-Q. Wu, Y.-Y. Zhu, B.-W. Wang and S. Gao, *Chinese J. Inorg. Chem.*, 2014, **30**, 1660; (d) A. Duerrbeck, S. Gorelik, J. Hobley, J. Wu, A. Hor and N. Long, *Chem. Commun.*, 2015, **51**, 8656.

15 (a) M. A. Halcrow, *Coord. Chem. Rev.*, 2009, **253**, 2493; (b) A. Galet, A. B. Gaspar, M. C. Muñoz and J. A. Real, *Inorg. Chem.*, 2006, **45**, 4413.

16 J. K. McCusker, A. L. Rheingold and D. N. Hendrickson, *Inorg. Chem.*, 1996, **35**, 2100.

17 M. Llunell, D. Casanova, J. Cirera, P. Alemany and S. Alvarez, *SHAPE*, version 2.0; Universitat de Barcelona: Barcelona, Spain, 2010.

18 M. A. Halcrow, *Chem. Soc. Rev.*, 2011, **40**, 4119.

19 P. Gütlich, V. Ksenofontov and A. B. Gaspar, *Coord. Chem. Rev.*, 2005, **249**, 1811.

20 R. L. Carlin, Magnetochemistry; Springer–Verlag Press: Berlin, Heidelberg, 1996.

21 (a) J. F. Letard, P. Guionneau and L. Goux-Capes, *Top. Curr. Chem.*, 2004, **225**, 221; (b) J. F. Létard, L. Capes, G. Chastanet, N. Moliner, S. Létard, J. A. Real and O. Kahn, *Chem. Phys. Lett.*, 1999, **313**, 115.

22 M. Baran, V. P. Dyakonov, L. Gladczuk, G. G. Levchenko, S. Piechota and G. Szymczak, *Physica C*, 1995, **241**, 383.

23 G. M. Sheldrick, *SHELXS-97*; University of Göttingen, Göttingen, Germany, 1990.

24 O. V. Dolomanov, L. J. Bourhis, R. J. Gildea, J. A. K. Howard and H. Puschmann, *J. Appl. Cryst.*, 2009, **42**, 339.

TOC

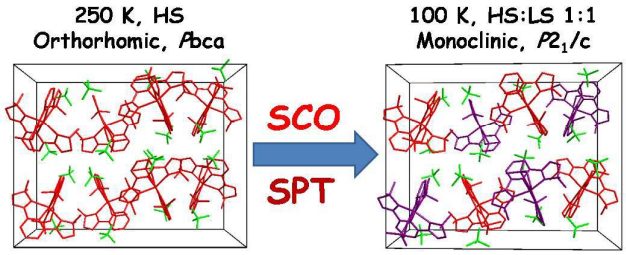

One mononuclear Fe^{II} complex displays a structural phase transition and a multi-induced spin-crossover behavior mediated by heat, light, pressure and solvent.